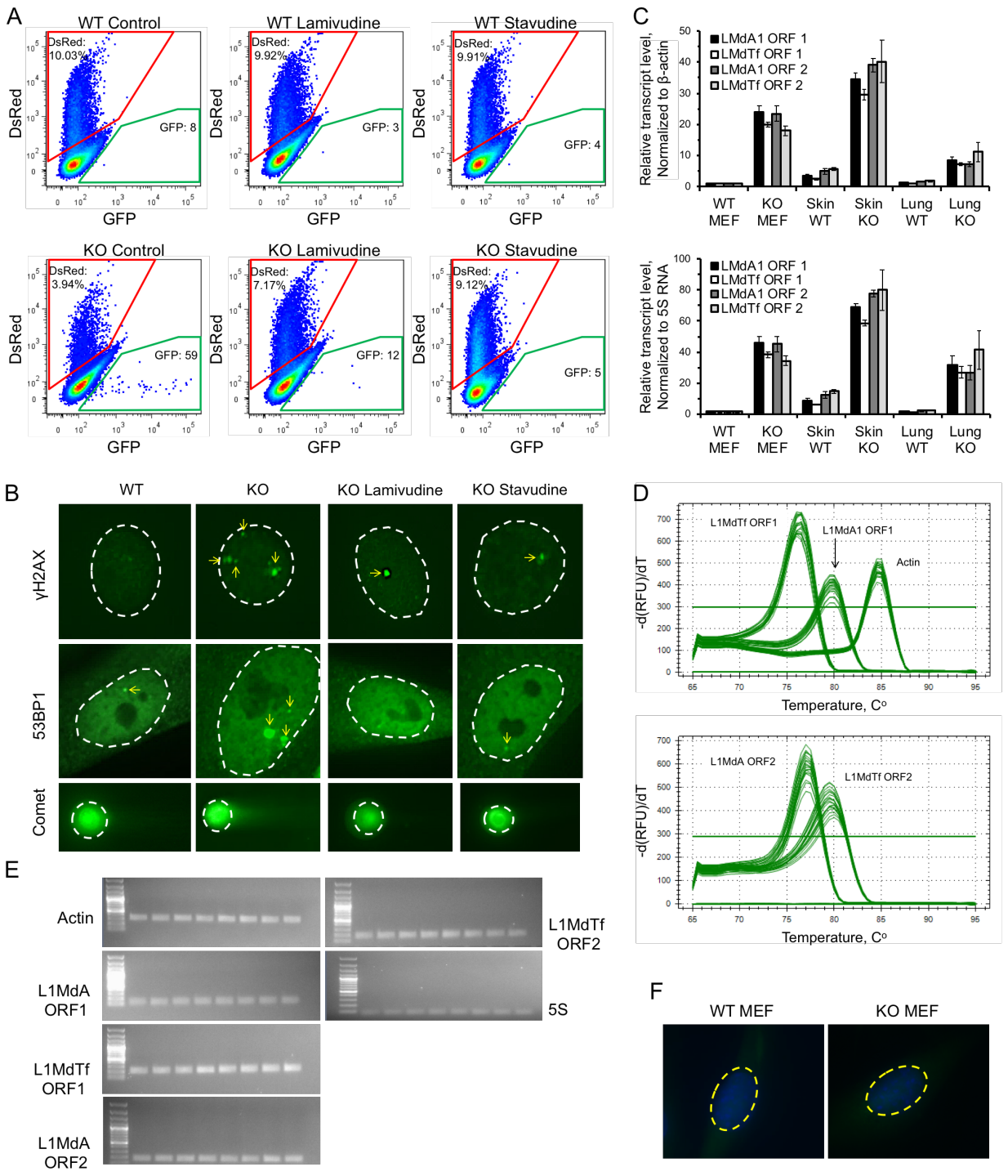

Figure S1. Related to Figure 1, 2 and 3 | Representative FACS traces for L1 EGFP reporter, primer validations, and representative images for γH2AX, 53BP1 immunostaining and comet assay.

A, Representative FACS traces from WT and SIRT6 KO MEFs transfected with mL1-EGFP reporter plasmid. A transfection control plasmid containing DsRed was used to standardize the retrotransposition activity with transfection efficiency.

B, Representative images for γH2AX, 53BP1 immunostaining and comet assay. Dashed white lines indicate the nucleus of the cells. Yellow arrows indicate foci for 53BP1 and γH2AX.

C, L1 qPCR primer validation. Two separate and active L1 families (L1MdA and L1MdTf) were probed using primers targeting sequences in both ORF1 and ORF2. Primers produced comparable trends in identical samples (both cell and tissue) normalized using both Actin and 5S RNA. The L1MdA1 ORF1 primer pair was used for all subsequent L1 quantifications.

D, L1 primer qRT-PCR melt peaks. Single peaks indicate specific target amplification and lack of primer dimers/off-target amplification.

E, Agarose gels of L1 qRT-PCR products post-amplification. All samples gave single bands at predicted amplicon length.

F, L1 DNA FISH staining controls treated with DNase. Samples were incubated with DNase prior to probe hybridization. Both WT and KO samples displayed reduced DAPI nuclear staining and complete lack of L1 FISH loci.

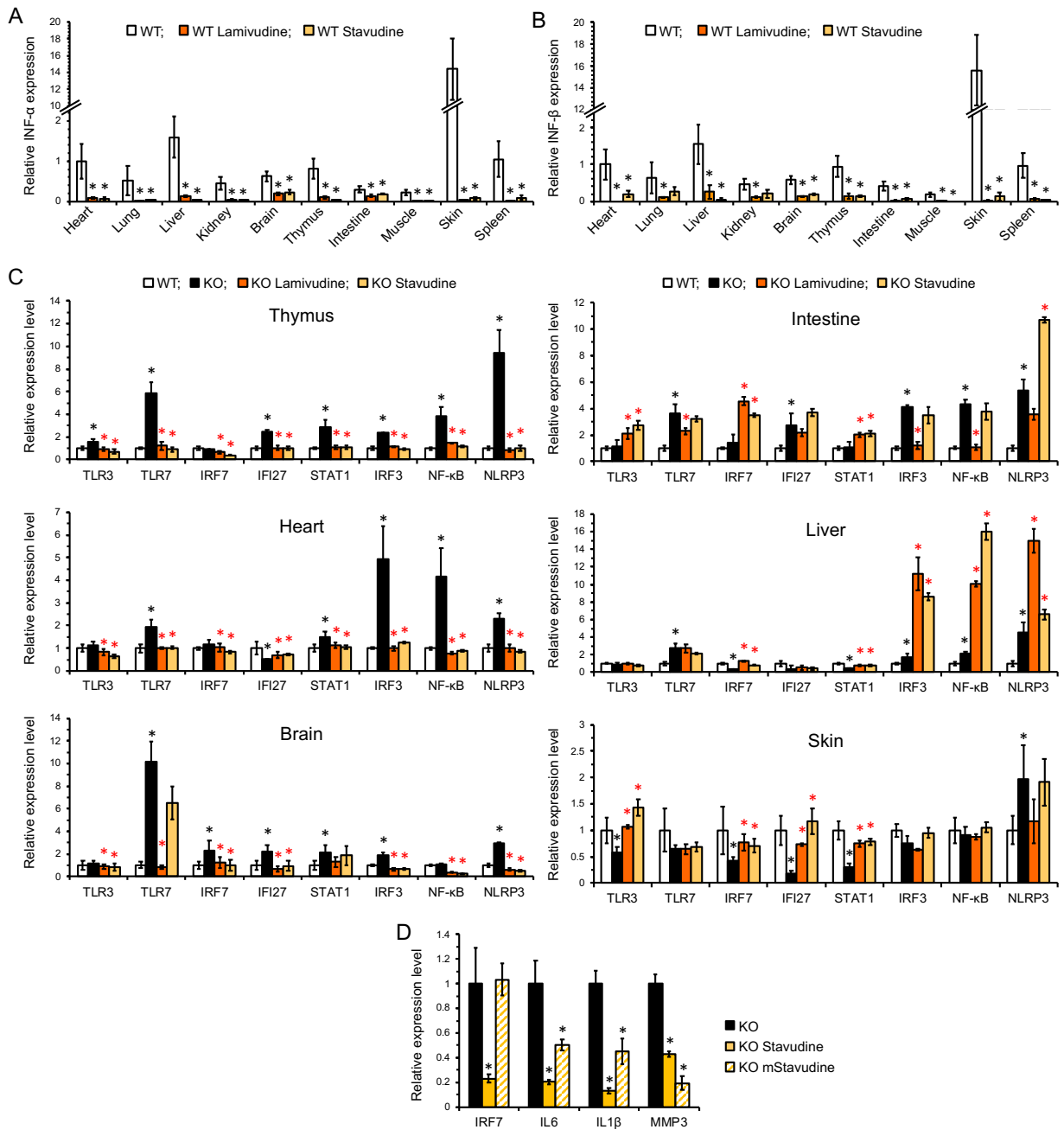

Figure S2. Related to Figure 4 | Expression of inflammation markers in tissues of mice treated with NRTIs.

A, B, NRTI treatment reduces basal levels of IFN-α/β in WT animals. The qRT-PCR values were normalized to actin and WT heart was used as a reference. Three animals were assayed for each group and error bars show s.d. Statistical significance was determined by the Student's *t*-test, asterisk indicates $p < 0.05$.

C, RT-qPCR analysis of inflammation genes in major organ systems was carried out on 27-day old animals. All values are relative expression levels compared to actin and then normalized to the WT. Data represents averages from five animals per treatment. Error bars show s.d. Statistical significance was determined by the Student's *t*-test. Black asterisks indicate significant differences from WT, and red asterisks indicate significant differences from water-treated SIRT6 KO, $p < 0.05$.

D, Methylated d4T (mD4T) does not impact INF response factors while still exhibiting anti-inflammatory activity on NLRP3 inflammasome factors. Error bars show s.d. Statistical significance was determined by the Student's *t*-test. Asterisks indicate significant differences from water-treated SIRT6 KO, $p < 0.05$.

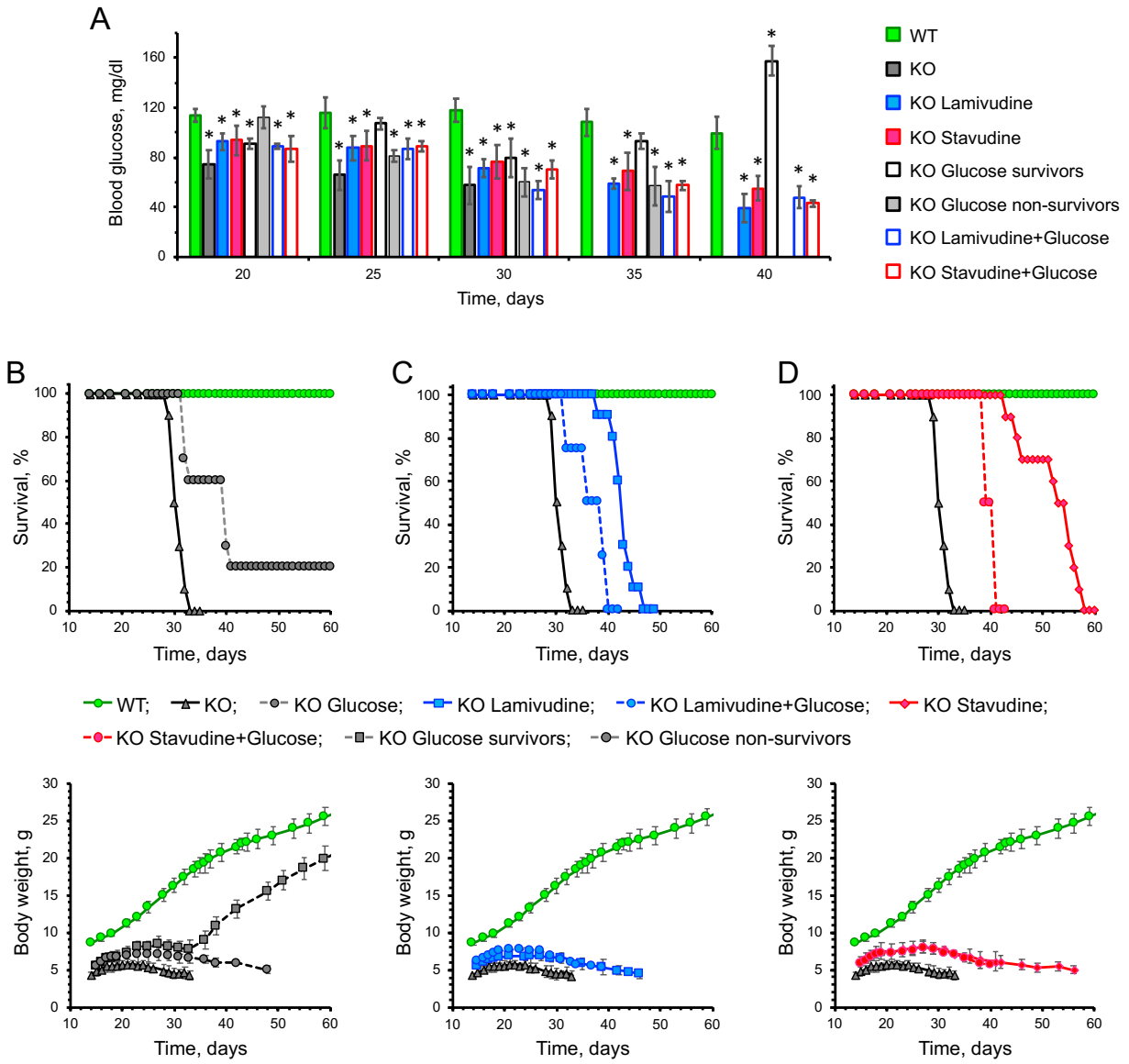

Figure S3. Related to Figure 5 | Glucose supplementation does not enhance NRTI impact on blood glucose, lifespan or bodyweight.

A, Blood glucose levels in NRTI-treated animals. NRTI treated animals still had low blood glucose at the time of weaning (day 22) compared to the WT, but slightly delayed further decline in blood glucose at day 30. Supplementation of 10% glucose in both control and NRTI treated animals did not significantly impact blood glucose levels. Five animals were assayed for each group and error bars indicate s.d. Asterisks indicate values significantly different from WT. Significance was determined by the paired *t*-test, $p < 0.05$.

B-D, Glucose supplementation does not improve NRTI rescue of SIRT6 KO mice lifespan or bodyweight. Control and NRTI-treated animals had diets supplemented with 10% glucose. A subset of control animals supplemented with glucose showed increased lifespan and bodyweight gain. NRTI-treated animals with glucose supplementation showed a significant decrease in lifespan compared to NRTI-only controls and no change in bodyweight. Ten animals were assayed for each group. Lifespans analyzed by log-rank and body weight by one-way ANOVA, $p < 0.05$.

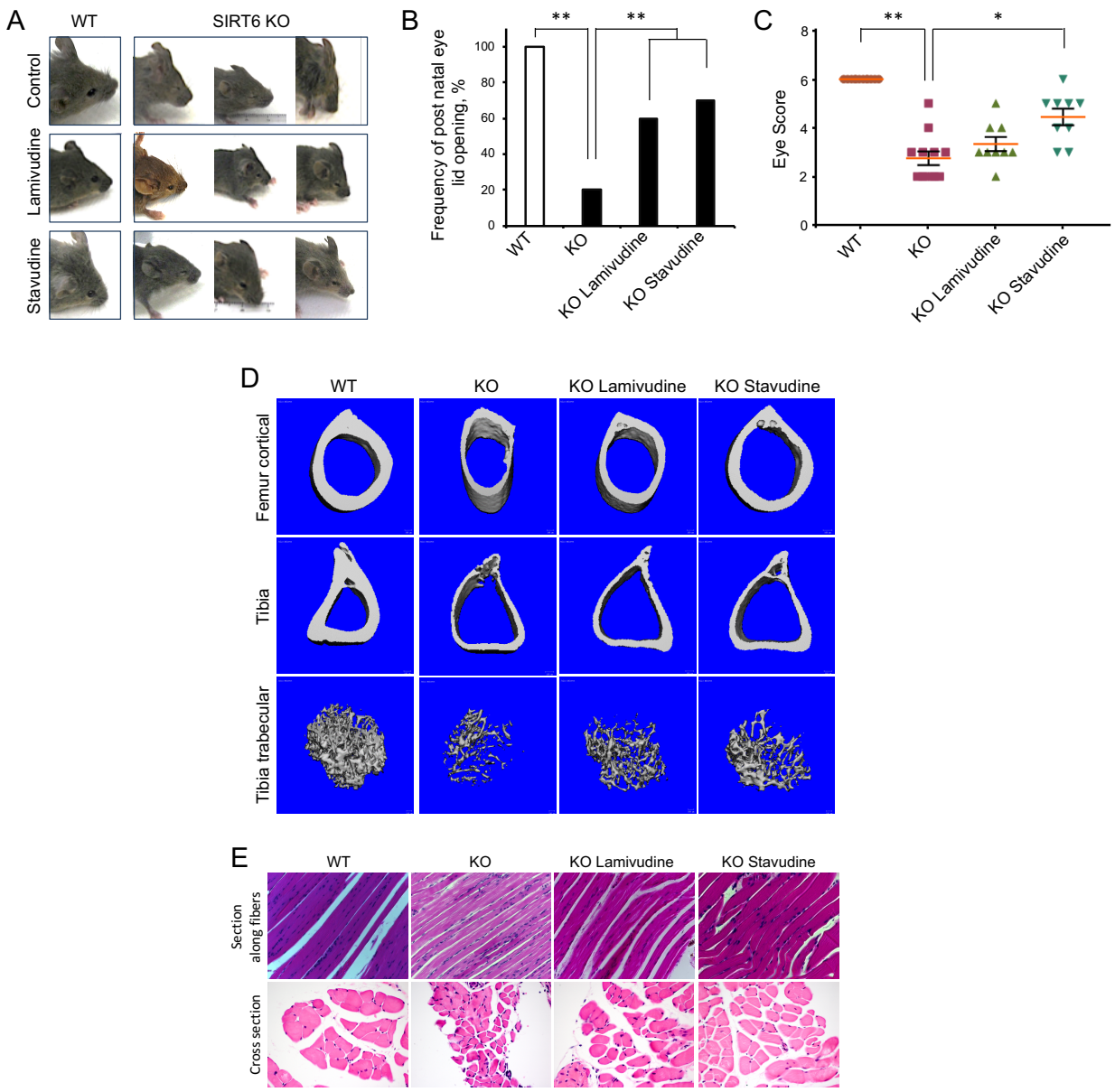

Figure S4. Related to Figure 5 | NRTI treatments improve SIRT6 KO physical robustness.

A, SIRT6 KO pups display a significantly reduced frequency of postnatal eyelid opening and their eyes remain closed until their death. Pups are pictured at 30 days old. 3TC and d4T treatment increased the frequency of eye opening in the SIRT6 KO mice.

B, Percentage of mice that opened their eyes by day 30. Ten mice were analyzed for each group. Double asterisk indicates $p < 0.0001$, Student t-test.

C, Individual animal eye scores. 1=fully closed, 2=partially open (some eyeball visible between eyelids), 3=fully open. Ten mice were analyzed for each group. Asterisk indicates $p = 0.001$, double asterisk indicates $p < 0.0001$, Student t-test.

D, Representative images of femur and tibia cross-sections and tibia trabecular (Figure 5G). Images were obtained by CT-scan of analysis of 27-day old animals.

E, Representative cross sections stained with Hematoxylin & Eosin of quadriceps of WT or KO NRTI-treated animals (Figure 5I).

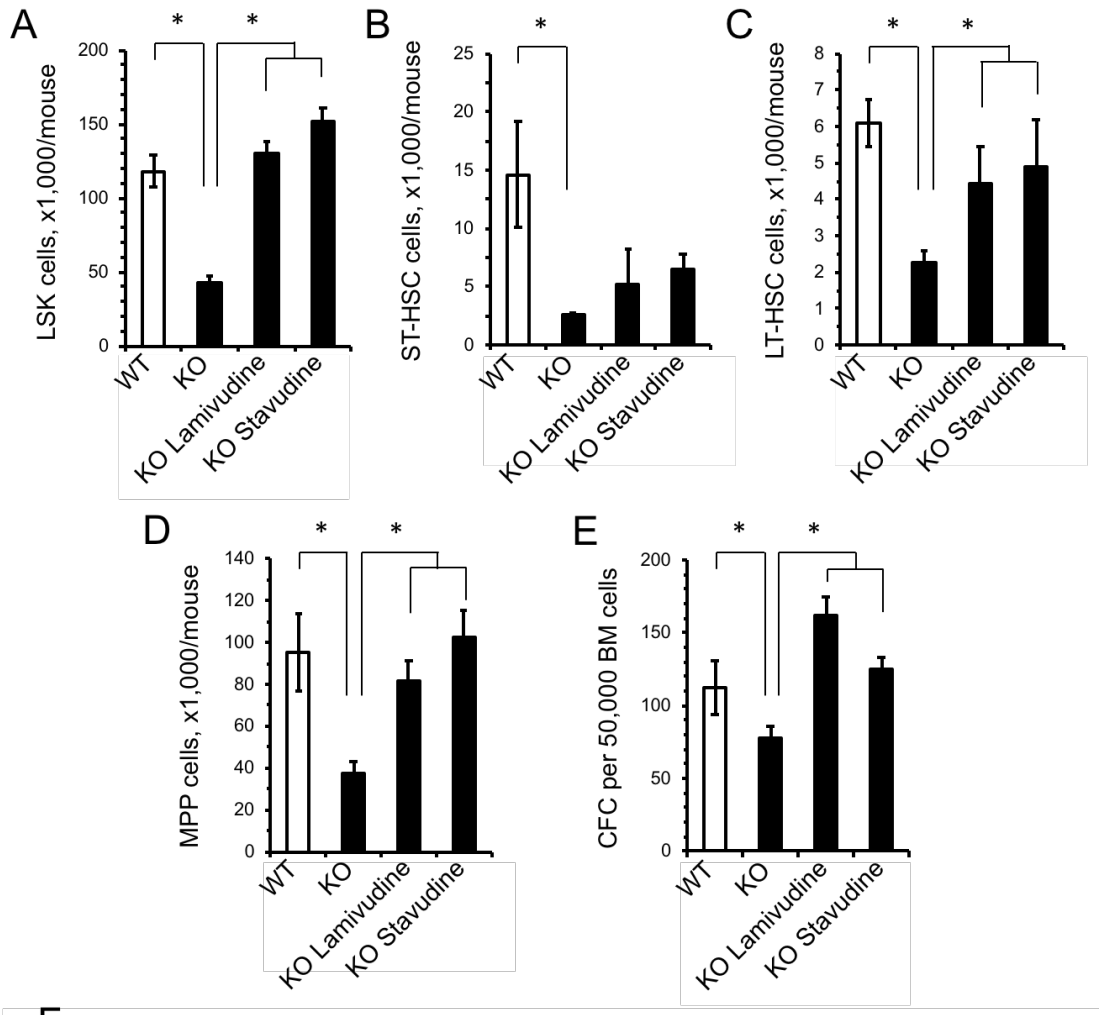
A
B
C
D
E
LSK cells, x1,000/mouse
ST-HSC cells, x1,000/mouse
LT-HSC cells, x1,000/mouse
MPP cells, x1,000/mouse
CFC per 50,000 BM cells
WT
KO
KO Lamivudine
KO Stavudine
*

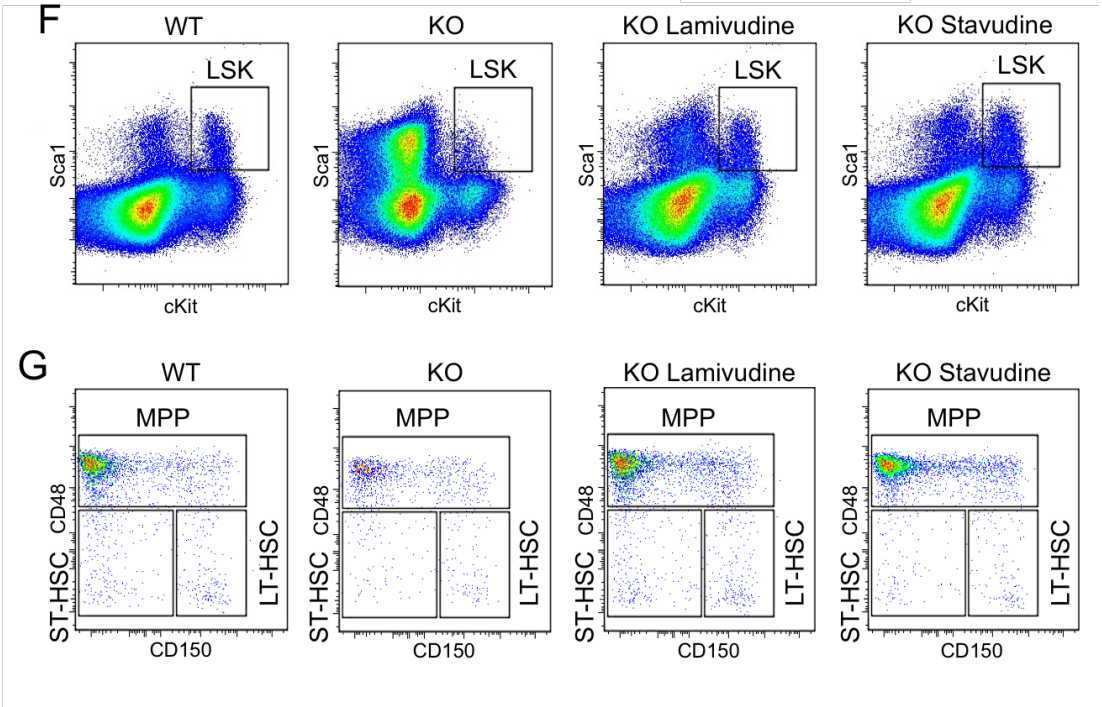
F
G
WT
KO
KO Lamivudine
KO Stavudine
LSK
Sca1
cKit
MPP
ST-HSC
LT-HSC
CD48
CD150

Figure S5. Related to Figure 5 | SIRT6 KO mice have reduced bone marrow stem cells populations and NRTI treatments increase the number of bone marrow stem cells.

A-D, The frequency of LSK, LT-HSCs ($Lin^-Sca1^+cKit^+CD48^-CD150^+$), ST-HSCs ($Lin^-Sca1^+cKit^+CD48^-CD150^-$), HSPCs ($Lin^-Sca1^+cKit^+$), and MPPs ($Lin^-Sca1^+cKit^+CD48^+CD150^-$) in the bone marrow was determined by flow cytometry. Flow cytometry plots are gated on Lin^- bone marrow cells. Data presented are the number of specified cell population per mouse.

E, The number of colonies formed in methylcellulose colony-forming assay using bone marrow cells from WT, SIRT6 KO, and NRTI-treated mice.

F, G, Representative flow cytometry analysis for Lin^- bone marrow cells from WT, SIRT6 KO, and NRTI-treated mice.

At least three animals were assayed for each group and error bars show s.d. Statistical significance was determined by the Student's *t*-test; asterisk indicate $p < 0.05$.

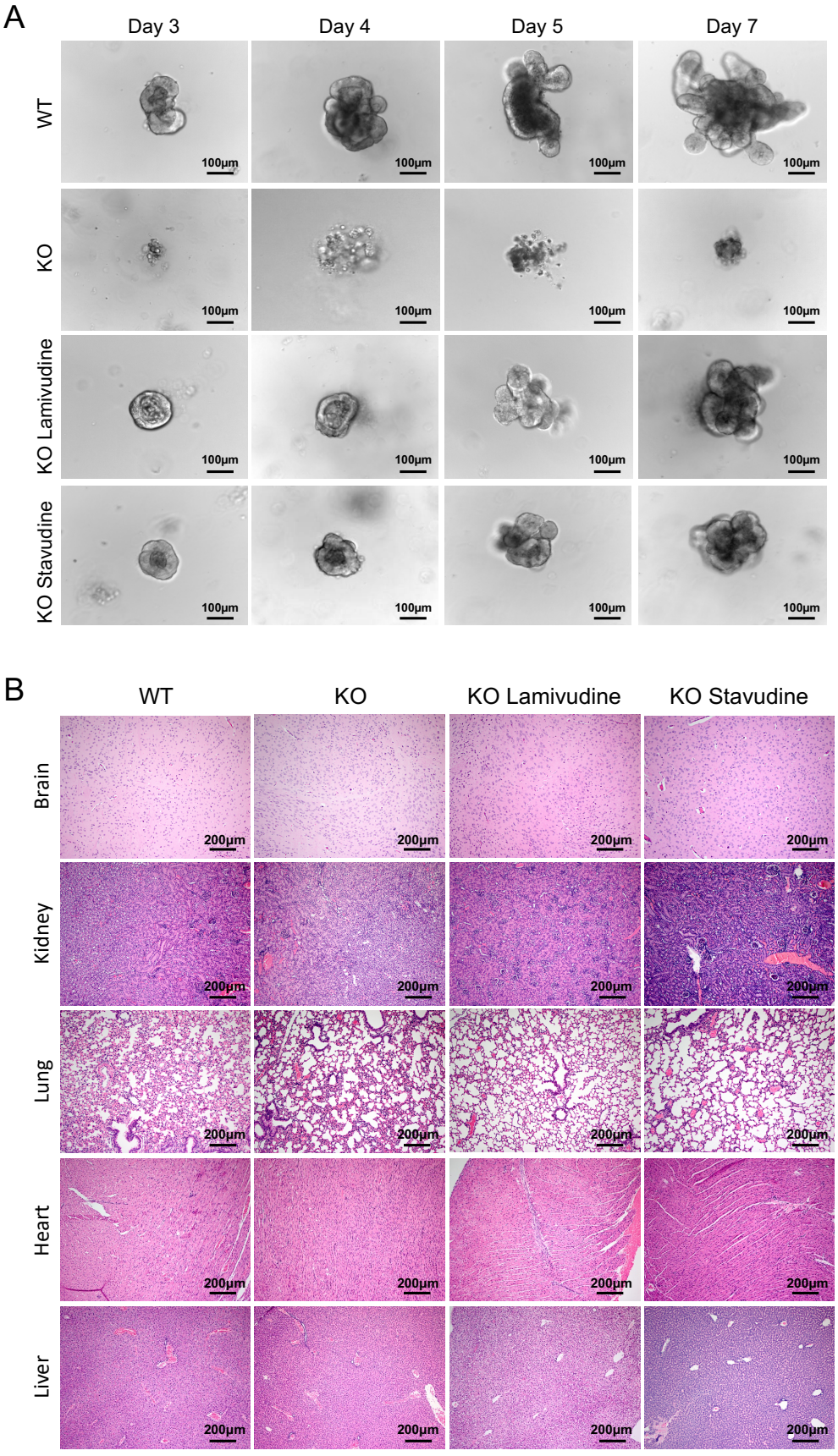
A
Day 3
Day 4
Day 5
Day 7
WT
KO
KO Lamivudine
KO Stavudine
100μm
B
WT
KO
KO Lamivudine
KO Stavudine
Brain
Kidney
Lung
Heart
Liver
200μm

Figure S6. Related to Figure 5 and Figure 6｜ Characterization of major organ systems of SIRT6 KO mice and effect of NRTI treatments.

A, NRTI treatments improve the ability of crypt cells from SIRT6 KO mice to form organoids *in vitro*. Crypt cells were isolated from 2 cm sections of mouse intestine and cultured in matrigel. WT crypts quickly gave rise to organoids and display distinct budding by day 7, whereas SIRT6 KO crypt cells showed little organoid development and often failed to form full organoids. NRTI-treated SIRT6 KO crypts displayed organoid growth and development, but with reduced budding compared to WT organoids.

B, Tissue histology for major organ systems in SIRT6 KO mice following NRTI treatment. All animals were euthanized at 27 days of age and tissues were immediately prepared for histology. Most tissues show little difference between WT, SIRT6 KO, and NRTI-treated animals. Images are representative of collected images from two animals per treatment. Tissues are hematoxylin & eosin stained at 100x magnification (scale bars = 200 μm).

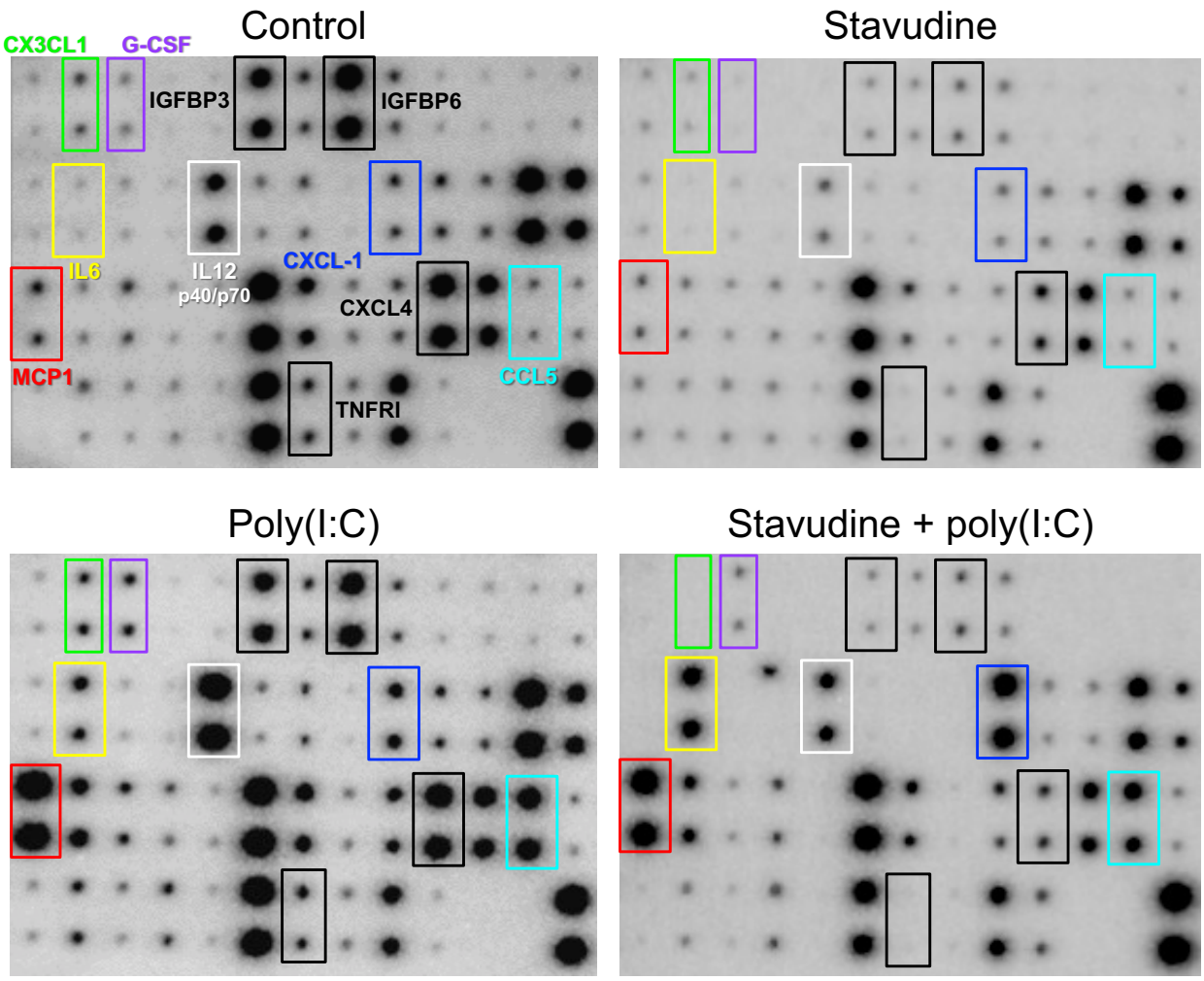

Fas ligand	CX3CL1	G-CSF	GM-CSF	IFNγ	IGFBP-3	IGFBP-5	IGFBP-6	IL-1α	IL-1β	IL-2	IL-3	IL-3 Rβ
IL-5	IL-6	IL-9	IL-10	IL-12 p40/p70	IL-12 p70	IL-13	IL-17A	KC (CXCL-1)	Leptin R	Leptin	LIX	L-Selectin
MCP-1 (CCL2)	MCP-5	M-CSF	MIG (CXCL9)	MIP-1α (CCL3)	MIP-1γ	MIP-2	MIP-3β (CCL19)	MIP-3α (CCL20)	PF-4 (CXCL4)	P-selectin	RANTES (CCL5)	CSF
TARC (CCL17)	I-309 (CCL1)	TECK (CCL25)	TIMP-1	TNF	TNF RI	TNF RII	TPO	VCAM-1	VEGF-A	blank	blank	Pos. control

Figure S7. Related to Figure 7 | Life-long d4T treatment reduces concentration of multiple cytokines and chemokines in plasma of aged WT mice. Wild type C57BL/6 mice were treated with 2 mg/ml d4T in drinking water since weaning. At 61 weeks of age, mice were treated with i.p.-injected poly(I:C), to induce type I interferon response. Control groups were injected with the vehicle (PBS). Blood was collected 6 hours post treatment equal volumes of plasma were

combined from two males and two females from each group for the detection of circulating cytokines and chemokines using Mouse Cytokine Antibody Array C3 kit. Factors that do not change their expression in response to poly(I:C) but are downregulated in d4T-treated mice are framed in black rectangles. A subset of factors induced by poly(I:C) and downregulated by d4T are framed in colored rectangles.

SUPPLEMENTAL TABLE 1: Related to Key Resource Table

Oligonucleotides	Source	Identifyer
mL1 ORF2 Fwd-ACAACACCCTTCTCAATAGTC	IDT	N/A
mL1 ORF2 Rev-CAGAAGATGGAAAGATCTCCC	IDT	N/A
L1MdTf ORF1 Fwd-GCCTACAGAACTCCAAATAGACTGG	IDT	N/A
L1MdTf ORF1 Rev-CCAGGCTCTTCTGGCTTTCATAG	IDT	N/A
L1MdTf ORF2 Fwd-GGTATGAAGAAACAAGCAGGAGTAG	IDT	N/A
L1MdTf ORF2 Rev-GGCTGCTCTTGTATTTGGAGCATAG	IDT	N/A
QuantumRNA Actin Universal primers	ThermoFisher	AM1720
iLenti L1 siRNA-TGGACCAGAAAAGAAATTCCTC	IDT	N/A
BLOCK-iT RNAi L1 Sequence #1-TCCAAATAGACTGGACCAGAA	IDT	N/A
BLOCK-iT RNAi L1 Sequence #2-AGAGCCTGGACAGATGTTATA	IDT	N/A
BLOCK-iT RNAi L1 Sequence #3-GAGGAGTAGACGGCAGGAAAT	IDT	N/A
BLOCK-iT RNAi L1 Sequence #4-TGGGATTAGTGCAGAGTTCTA	IDT	N/A
BLOCK-iT RNAi L1 Sequence #5-CCATACTTATCTCCTTGTACT	IDT	N/A
IRF7 Fwd-AAACCATAGAGGCACCCAAG	IDT	N/A
IRF7 Rev-ACAGGCAGTCTGGGAGAATC	IDT	N/A
IRF127 Fwd-CTCTGGCACCATTCTAGCTG	IDT	N/A
IRF127 Rev-GTGCTCCAAGTGCAGATGTT	IDT	N/A
STAT1 Fwd-ATTCAGAGCTCCTTCGTGGT	IDT	N/A
STAT1 Rev-TCAGCTCTTGCAATTTCACC	IDT	N/A
TLR3 Fwd-AACTGCCTGAATCACAATCG	IDT	N/A
TLR3 Rev-ATTATGGGTGCAATCCCTGT	IDT	N/A
TLR7 Fwd-TCTCTCCAGATTCCTTCCGT	IDT	N/A
TLR7 Rev-TCTGCAGCCTCTTGGTACAC	IDT	N/A
NFKB Fwd-GCTGGAAATTCCTGATCCAGACA	IDT	N/A
NFKB Rev-ATCACTTCAATGGCCTCTGTGTAG	IDT	N/A
NLRP3 Fwd-AGAGCCTACAGTTGGGTGAAATG	IDT	N/A
NLRP3 Rev-CCACGCCTACCAGGAAATCTC	IDT	N/A
IRF3 Fwd-GATGGAGAGGTCCACAAGGAC	IDT	N/A
IRF3 Rev-GACCATCACAAGCCTCTTGACC	IDT	N/A
IL6 Fwd-CGGAGAGGAGACTTCACAGAGGA	IDT	N/A
IL6 Rev-TTTCCACGATTTCCCAGAGAACA	IDT	N/A
IL1β Fwd-CCGTGGACCTTCCAGGATGA	IDT	N/A
IL1β Rev-GGGAACGTCACACACCAGCA	IDT	N/A
MMP3 Fwd-GACTCAAGGGTGGATGCTGT	IDT	N/A
MMP3 Rev-CCAACTGCGAAGATCCACTG	IDT	N/A
L1 ORF1 FISH AlxFlu488-	IDT	N/A

CTTCACATAAAACCAGAGACACTG-AlxFlu488		
L1 ORF2 FISH AlxFlu488-CACCAGTGAGAATGGCTAAGATC-AlxFlu488	IDT	N/A
GAPDH FISH AlxFlu488-GGCATGGCCTTCCGTGTTCCTAC-AlxFlu488	IDT	N/A
cGAS RNAi	Ambion	s103166
cGAS RNAi	Ambion	s103167
cGAS RNAi	Ambion	s103168
Silencer Select Negative Control 1	Ambion	4390843